IEEE Access
Multidisciplinary ⋮ Rapid Review ⋮ Open Access Journal

Received November 21, 2019, accepted December 7, 2019, date of publication December 13, 2019,
date of current version February 11, 2020.

*Digital Object Identifier 10.1109/ACCESS.2019.2959274*

# Direction-of-Arrival Estimation Under Array Sensor Failures with ULA

**BING SUN[1], CHENXI WU[1], JUNPENG SHI[1], HUAI-LIN RUAN[1], AND WEN-QIANG YE[2]**
[1]College of Electronic Engineering, National University of Defense Technology, Hefei 230037, China
[2]Satellite Control Center, Xi'an 710043, China

Corresponding author: Chenxi Wu (wuchenxi19881201@126.com)

This work was supported in part by the National Natural Science Foundation of China under Grant 61171170, and in part by the Natural Science Foundation of Anhui Province under Grant 1408085QF115 and Grant 1908085QF280.

**ABSTRACT** In this paper, to address the problem of array sensors failure, we propose a covariance matrix reconstruction method for direction-of-arrival (DOA) estimation. Firstly, we devise a diagnosis method to detect and locate the positions of failure sensors. According to the robustness of the array, the sensor failure scenarios are classified into redundant sensors failure and non-redundant sensors failure. Then, the corresponding DOA estimation method is adopted for two failure scenarios. The former can be solved using the virtual sensors in the difference coarray. As for the latter, the difference coarray has some holes, resulting in the decrease of available continuous virtual sensors or degrees of freedom (DOFs). Based on the matrix completion theory, the covariance matrix is extended to a high-dimensional Toeplitz matrix with missing data, where some elements are zero. We employ the mapping matrix, further use trace norm instead of the rank norm for convex relaxation to reconstruct the covariance matrix, thereby realizing the filling of the virtual sensor holes in difference coarray and restoring the DOFs. Compared with the sparsity-based methods, the proposed method can eliminate the effect of the discretization of the angle domain, and avoid regularization parameter selection. Finally, the root-MUSIC method is given for DOA estimation. Theoretical analysis and simulation results show that the proposed methods can alleviate the effect of array sensors failure and improve the estimation performance.

**INDEX TERMS** Direction of arrival (DOA), sensor failure, difference coarray, matrix reconstruction, redundant sensors.

## I. INTRODUCTION

Direction of Arrival (DOA) estimation has a wide range of applications in digital communication, signal processing, and target detection, and is one of the core research contents in the field of array signal processing [1]–[4]. A large number of high-resolution methods have been proposed under the circumstances of array sensors intact, and some methods [5]–[9] even have strict requirements for the array configurations. Recently, the research in [10], [11] reveal that the coarray structures of sparse arrays are susceptible to sensors failure, which can result in a reduction of the degrees of freedom (DOFs) [12]–[15], and may also cause the failure of the entire system. In real scenarios, the phased array has large number of sensors, which are affected by harsh natural environment, electromagnetic interference, component aging, physical damage, etc., and consequently increase the probability of sensors failure.

The numbers and positions of failure sensors have different effects on DOA estimation performance, as proposed in [10], [11]. In this case, it is crucial to detect and locate the positions of the failure sensors and take remedial action to restore the DOA estimation performance [16]–[19]. The authors in [10], [11] propose a theory quantitatively analyze the robustness of intact array by introducing the k-essentialness of sensors and $k$-essential family of arrays. From the analysis for the uniform linear array (ULA), it can be seen that the situation is relatively complicated when $k$ takes different values, but it is necessary for robustness analysis. In this paper, we aim to address the DOA estimation problem under the sensors failure scenarios. After detecting and locating the failure sensors, it is not necessary to classify the failure sensors using the $k$-essentialness of sensors and $k$-essential family of arrays. We classify failure sensors into redundant sensors and non-redundant sensors based on the numbers and positions

The associate editor coordinating the review of this manuscript and approving it for publication was Manuel Rosa-Zurera.

of failure scenarios. The impact of failure sensors on DOA estimation is analyzed in a deterministic fashion. This classification is also applicable to redundant sensors such as ULA, coprime array, nested array, etc.

For handling sensors failure, many modifications for conventional methods are proposed. A neural network method is used to train the data model through the neural algorithm to recover the missing data of the covariance matrix under the sensors failure [20]. However, this method relies entirely on prior knowledge, thus limiting its application in practical engineering. In [21], [22], the authors use an iterative method for sensors failure diagnosis and consequently may converge slowly, especially when the matrix is ill-conditioned. The study in [23]–[25] restores the original antenna array by reoptimizing the amplitude excitation of the remaining intact sensors, thereby solving the practical problem of the linear array sensors failure. However, this method only changes the weight coefficient of the remaining intact sensors, and cannot restore the original DOFs of the array. The covariance matrix reconstruction method proposed in [26] recovers the corresponding missing elements by the normal covariance matrix elements. However, this method is only applicable to the DOA estimation of multiple-input multiple-output (MIMO) radar sensors failure when the transmission and reception sensors spacing meets a specific relationship. In a recent contribution [27], authors address problem of partial sensors failure by replacing the failure sensors with the virtual sensors in difference coarray. But the positions of failure sensors are not considered.

In view of the above problems, we devise a diagnosis method to detect and locate the positions of failure sensors according to the distribution characteristics of the elements in the covariance matrix. The sensor failure scenarios are classified into redundant sensors failure and non-redundant sensors failure. Then, we propose two DOA estimation approaches for the redundant and non-redundant sensors failure. The former can be solved using the virtual sensors in difference coarray to replace the failure sensors. As for the latter, the virtual sensors in difference coarray will have holes [28], [29], and the number of available continuous virtual sensors will decrease, resulting in loss of DOFs. Based on the matrix completion theory [30]–[32], the covariance matrix is extended to a high-dimensional Toeplitz matrix with missing data, of which some elements are zero. We employ the mapping matrix, further use trace norm instead of the rank norm for convex relaxation to recover the matrix, thereby realizing the filling of the holes in difference coarray and restoring the DOFs. Compared with the sparsity-based method, the proposed method can eliminate the effect of the off-grid without discretization of the angle domain, and avoid regularization parameter selection. Finally, the root-MUSIC method is employed for the DOA estimation. The proposed method can alleviate the effect of the decrease of the DOFs caused by the array sensor failures. Therefore, the estimation accuracy is improved.

To be clear, the main contributions of this paper are given as follows.

- We devise a diagnosis method to detect and locate the positions of failure sensors, which can be employed for suppressing the DOA estimation performance degradation as shown in [10], [11].
- We classify failure sensors into redundant sensors and non-redundant sensors based on the positions of failure scenarios. The impact of failure sensors on DOA estimation is analyzed in a deterministic fashion. Additionally, this classification is also applicable to redundant sensors such as ULA, coprime array, nested array, etc.
- In the case of non-redundant sensors failure, based on the matrix completion theory, we employ the mapping matrix, and further use trace norm instead of the rank norm for convex relaxation to recover the matrix, thereby realizing the filling of the holes in difference coarray and restoring the DOFs.

The remainder of the paper is arranged as follows. Section 2 deals with the diagnosis and classification of failures. In Section 3, a covariance matrix reconstruction DOA estimation method is proposed in sensors failure scenarios. In Section 4, numerical simulations and the corresponding discussions are given to verify the effectiveness of the proposed algorithm. Finally, Section 5 draws the conclusions for this paper.

Notations used in this paper are as follows. The lower-case and upper-case bold characters denote vectors and matrices. $(\cdot)^T$, $(\cdot)^*$ and $(\cdot)^H$ represent transpose, conjugation, and conjugate transpose, respectively. $\cdot$ and $\otimes$ represent Hadamard product and Kronecker product, respectively. tr$(\cdot)$, rank$(\cdot)$ are the trace and rank operators, respectively. $\boldsymbol{I}_N$ denotes $N \times N$ identity matrix. $diag(\cdot)$ denotes the diagonal matrix operator. $|\cdot|$ denotes the absolute value operator. $\|\cdot\|_2$ denotes $\ell_2$-norm. $\boldsymbol{E}[\cdot]$ and $vec(\cdot)$ denote expectation and vectorization operator, respectively.

## II. FAILURE SENSOR DIAGNOSIS AND CLASSIFICATION

In this paper, we mainly discuss the ULA failure scenarios, which is the most common array configuration. In principle, the theory in this paper can be used to analyze sensor failures in other array models, but the details will be very complicated. Due to page limitations, the analysis of these array models will be left for further study.

The ULA contains $N$ physical sensors. The unit spacing between two consecutive elements is $d_0 = \lambda/2$, where $\lambda$ is the wavelength of carrier frequency. Assuming that $K$ coplanar far-field narrowband sources impinging on the array from the directions $\boldsymbol{\theta} = [\theta_1, \theta_2, \cdots, \theta_K]$, the array output is expressed as:

$$\boldsymbol{X}(t) = \boldsymbol{A}\boldsymbol{S}(t) + \boldsymbol{N}(t) \tag{1}$$

where $\boldsymbol{X}(t) = [x_1(t), x_2(t), \cdots, x_N(t)]^{\mathrm{T}}$ is the output of array, $\boldsymbol{S}(t) = [s_1(t), s_2(t), \cdots, s_K(t)]^T$ is the signal waveforms of each source, $\boldsymbol{N}(t) = [n_1(t), n_2(t), \cdots, n_N(t)]^{\mathrm{T}}$

denotes the white Gaussian noise vector, and $\boldsymbol{A} = [\boldsymbol{a}(\theta_1), \boldsymbol{a}(\theta_2), \cdots, \boldsymbol{a}(\theta_K)]$ is manifold matrix with $\boldsymbol{a}(\theta_k) = [1, e^{j\frac{2\pi d_0}{\lambda}\sin\theta_k}, \cdots, e^{j\frac{2(N-1)\pi d_0}{\lambda}\sin\theta_k}]^{\mathrm{T}}$ being the steering vector.

We assume that the impinging signals are independent and uncorrelated, the covariance matrix of the output data can be given as:

$$\begin{aligned}\boldsymbol{R} &= \boldsymbol{E}\left\{\boldsymbol{X}(t)\boldsymbol{X}(t)^{\mathrm{H}}\right\} \\ &= \boldsymbol{A}\begin{bmatrix}\sigma_1^2 & & & \\ & \sigma_2^2 & & \\ & & \ddots & \\ & & & \sigma_K^2\end{bmatrix}\boldsymbol{A}^{\mathrm{H}} + \sigma_n^2\boldsymbol{I}\end{aligned} \tag{2}$$

where $\sigma_k^2$ is the power of the $k$th impinging signal, and $\sigma_n^2$ denotes the noise power.

If the array sensor fails, we assume it is completely faulty and cannot get any useful information. If the $i$th sensor fails, all elements on the $i$th row of the manifold matrix $\boldsymbol{A}$ are replaced with 0. Therefore, the elements in the $i$th row and the $i$th column of the covariance matrix $\boldsymbol{R}$ are all 0 except for the diagonal elements.

Taking the ULA contains the $N$ physical sensors as an example. We assume that the second sensor fails and all elements on the second row of the manifold matrix $\boldsymbol{A}_1$ are replaced with 0. The manifold matrix $\boldsymbol{A}_1$ is expressed as:

$$\boldsymbol{A}_1 = \begin{bmatrix} 1 & 1 & \cdots & 1 \\ 0 & 0 & \cdots & 0 \\ e^{j\frac{4\pi d_0}{\lambda}\sin\theta_1} & e^{j\frac{4\pi d_0}{\lambda}\sin\theta_2} & \cdots & e^{j\frac{4\pi d_0}{\lambda}\sin\theta_K} \\ \vdots & \vdots & \ddots & \vdots \\ e^{j\frac{2(N-1)\pi d_0}{\lambda}\sin\theta_1} & e^{j\frac{2(N-1)\pi d_0}{\lambda}\sin\theta_2} & \cdots & e^{j\frac{2(N-1)\pi d_0}{\lambda}\sin\theta_K} \end{bmatrix} \tag{3}$$

Substituting (3) into to (2), we can formulate the covariance matrix as:

$$\boldsymbol{R}_1 = \begin{bmatrix} \sum_{k=1}^{K}\sigma_k^2 + \sigma_n^2 & 0 & \sum_{k=1}^{K}\sigma_k^2 e^{-jB} & \cdots & \sum_{k=1}^{K}\sigma_k^2 e^{-jF} \\ 0 & \sigma_n^2 & 0 & \cdots & 0 \\ \sum_{k=1}^{K}\sigma_k^2 e^{jB} & 0 & \sum_{k=1}^{K}\sigma_k^2 + \sigma_n^2 & \cdots & \sum_{k=1}^{K}\sigma_k^2 e^{-jG} \\ \vdots & \vdots & \vdots & \ddots & \vdots \\ \sum_{k=1}^{K}\sigma_k^2 e^{-jF} & 0 & \sum_{k=1}^{K}\sigma_k^2 e^{jG} & \cdots & \sum_{k=1}^{K}\sigma_k^2 + \sigma_n^2 \end{bmatrix} \tag{4}$$

where $B = \frac{4\pi d_0}{\lambda}\sin\theta_k$, $F = \frac{2(N-1)\pi d_0}{\lambda}\sin\theta_k$, $G = \frac{2(N-3)\pi d_0}{\lambda}\sin\theta_k$. Under ideal assumptions, if the row and column elements of $\boldsymbol{R}_1$ have only unique non-zero elements, we can determine that there is a failure sensor. However, in real scenarios, the sampling noise is not the ideal Gaussian white noise, and the noise covariance matrix is non-diagonal. Signals and noise are not completely uncorrelated. If there are sensor failures, there are no rows and columns in $\boldsymbol{R}_1$ whose elements are all zero elements except for the diagonal ones. Therefore, we propose a detection algorithm to diagnose the failure sensors and their positions.

In the case of sensors failure, the covariance matrix $\hat{\boldsymbol{R}}$ of the actual array output data is compared to the ideal covariance matrix $\boldsymbol{R}$. The zero elements on the rows and columns of $\boldsymbol{R}$ corresponding to the failure sensor are replaced by the signal and noise cross-correlation term and the cross-correlation term of the noise received by different sensors. The sum of the absolute values of the rows corresponding to the failure sensors is significantly smaller than the mean of the sum of the absolute values of the rows corresponding to the other non-failure sensors, the columns are also the same. Therefore, the sensors failure can be diagnosed by the following formula as:

$$\begin{cases} r(i,:) \le \gamma\dfrac{1}{N}\displaystyle\sum_{i=1}^{N} r(i,:) \\ r(:,j) \le \gamma\dfrac{1}{N}\displaystyle\sum_{j=1}^{N} r(:,j) \end{cases} \tag{5}$$

where $r(i,:) = \sum_{j=1}^{N}\left|\hat{R}(i,j)\right|$ is the sum of the absolute values of the rows of $\hat{\boldsymbol{R}}$. $r(:,j) = \sum_{i=1}^{N}\left|\hat{R}(i,j)\right|$ is the sum of the absolute values of the columns of $\hat{\boldsymbol{R}}$. $\gamma$ is the detection threshold factor that ranges from 0 to 1. $\gamma$ has to be chosen properly since a smaller $\gamma$ may discard the failure sensors while a larger $\gamma$ may bring in spurious failure sensors, both of which can deteriorate the performance of failure sensor diagnosis. In the experiment, we verified the diagnosis performance of different $\gamma$ values in steps of 0.1. In this paper, we give the empirical value $\gamma = \begin{cases} 0.5, \text{if} -15\text{dB} < \text{SNR} \le 0\text{dB} \\ 0.4, \text{if SNR} > 0\text{dB} \end{cases}$ based on the experimental results, which gives good performance empirically. If $r(i,:)$ and $r(:,j)$ satisfy (5) at the same time, and $i = j$, the $i$th sensor fails.

The different numbers and positions of failure sensors have crucial effects on DOA estimation performance, and also determine the choice of DOA estimation methods for sensors failure scenarios. Therefore, we classify different cases of array sensor failure. In this paper, we classify the failure sensors into redundant sensors and non-redundant sensors based on array redundancy.

To better understand, we briefly review the difference coarray. The set is defined as:

$$D = \{d_n - d_{n'}\},\ d_n, d_{n'} \in C \tag{6}$$

where $C$ is the set of array sensor positions. $d_n$, $d_{n'}$ are the positions of different physical sensors. $D$ is the set of differences between the positions of physical sensors, where the same elements exist, and the set of all the different position differences $d_u$ is defined as $D_u$. The frequency of $d_u$ in set $D$ is defined as the weight coefficient $\omega_d(d_u)$. The $(m,p)-$ th element of the covariance matrix $\boldsymbol{R}$ may be interpreted as an aggregated signal received from all sources observed at a virtual element located at $d_m - d_p$. We regard virtual element as virtual sensor.

**Algorithm 1** Proposed Algorithm for Failure Sensor Diagnosis and Classification

**Step 1:** Calculate the array output data covariance matrix $\hat{\boldsymbol{R}}$.

**Step 2:** Calculate the sum of the absolute values of the rows $r(i,:) = \sum_{j=1}^{N} \left|\hat{R}(i,j)\right|$ and calculate the sum of the absolute values of the columns $r(:,j) = \sum_{i=1}^{N} \left|\hat{R}(i,j)\right|$.

**Step 3:** Determine whether $r(i,:)$ and $r(:,j)$ satisfy (5), and $i = j$. If (5) is satisfied, the $i$th sensor fails, otherwise the $i$th sensor does not fail.

**Step 4:** Calculate position difference set $D = \{d_n - d_{n'}\}$ of the intact sensors.

**Step 5:** Remove the same position differences to get the set $D_u$, and obtain the number of consecutive virtual sensors $Q$.

**Step 6:** If $Q = 2N - 1$, the redundant sensors fail, otherwise the non-redundant sensors fail.

The positions of the failure sensors are known, and the positions difference set $D$ are obtained from (6) for the remaining intact sensors. Then, the same position differences are removed to obtain the set $D_u$, and the numbers of consecutive virtual sensors $Q$ is obtained. The numbers of consecutive virtual sensors in the intact array is $2N - 1$. If $Q = 2N - 1$, the redundant sensors fail, otherwise the non-redundant sensors fail. For failure sensors diagnosis and classification, We show the main steps of the proposed method as follows

For ULA with $N$ sensors, the sensor location set is $\{0, 1, \cdots, N-1\}$. We classify the sensors into redundant sensors and non-redundant sensors. To simplify the discussion, we give non-redundant sensors expressions:

$$\psi_1 = \begin{cases} \{\{0\}\}, & \text{if } N = 1, \\ \{\{0\},\{1\}\}, & \text{if } N = 2, \\ \{\{0\},\{1\},\{2\}\}, & \text{if } N = 3, \\ \{\{0\},\{N-1\}\}, & \text{if } N > 3, \end{cases} \tag{7}$$

$$\psi_2 = \begin{cases} \emptyset, & \text{if } 1 \le N \le 3, \\ \{\{1,2\}\}, & \text{if } N = 4, \\ \{\{1,2\},\{1,3\},\{2,3\}\} & \text{if } N = 5, \\ \{\{1,4\},\{2,3\}\}, & \text{if } N = 6, \\ \{\{1,N-2\}\}, & \text{if } N > 6, \end{cases} \tag{8}$$

$$\psi_3 = \begin{cases} \emptyset, & \text{if } N \le 6, \\ \{\{1,2,3\},\{1,2,4\},\{2,3,4\}, \\ \quad \{2,4,5\},\{3,4,5\}\}, & \text{if } N = 7, \\ \{\{1,2,5\},\{2,3,4\}, \\ \quad \{2,5,6\},\{3,4,5\}\}, & \text{if } N = 8, \\ \{\{1,2,6\},\{2,6,7\},\{3,4,5\}\} & \text{if } N = 9, \\ \{\{1,2,N-3\},\{2,N-3,N-2\}\} & \text{if } N > 9, \end{cases} \tag{9}$$

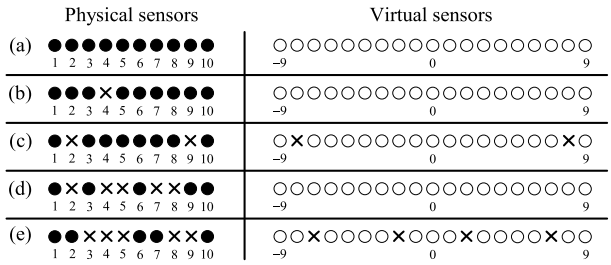


**FIGURE 1.** The positions of the physical sensors and the virtual sensors in difference coarray of different failure scenarios. Physical sensors are marked by solid circles and the virtual sensors are marked by hollow circles, while the failure sensors and holes are depicted by crosses. (a) the intact ULA array, (b) the 4th sensor failure, (c) the 2nd and 9th sensors failure, (d) the 2nd, 4th, 5th, 7th, and 8th sensors failure and (e) the 3rd, 4th, 5th, 8th, and 9th sensors failure.

where $\psi_k$ represents the set of locations for $k$ non-redundant sensors. Note that for $\psi_{k_1}$ and $\psi_{k_2}$, if $k_1 < k_2$, $k_1$ non-redundant sensors in $\psi_{k_1}$ will not be repeated in $\psi_{k_2}$. This is because $k_1$ non-redundant sensors combined with other $k_2 - k_1$ arbitrary position sensors are necessarily non-redundant.

Note that the sensors at both ends of array are more important than others. It was shown in [33] that for the ULA with 6 sensors, the position set is {0,1,2,3,4,5}, the sensors at 0 and 5 are more important than sensors at 1, 2, 3, and 4. According to the Theorem 2 in [11], the sensors at 0 and $N-1$ are the most essential ones while the others are inessential. To simplify the discussion, we make the following additional assumptions: If the positions of failure sensors are at the ends of the array, the maximum DOFs that can be recovered is the maximum DOFs of the remaining ULA after removing the endpoint sensors.

If there are multiple failure sensors, the influence on difference coarray becomes more complicated. Taking a uniform linear array with 10 sensors as an example, if only one sensor fails and its position is anywhere except for the two endpoints, we can use the redundancy of the array to fill the position of the failure sensor. If the two sensors fail, only when the 2nd sensor and the 9th sensor fail simultaneously, the redundancy of the remaining sensors cannot restore the original DOFs, and any other two sensors failure can be addressed by redundancy. The ULA with 10 sensors can recover the DOFs in the case of a maximum of 5 failure sensors. For example, the 2nd, 4th, 5th, 7th, and 8th array sensors fail, and the remaining intact sensors constitute the minimum redundant array, and the difference coarray can restore the original DOFs. Figure 1 shows the positions of the physical sensors and the virtual sensors in difference coarray of different failure scenarios.

Figure 1a shows intact ULA array. Figure 1b and 1d shows redundant sensors failure. Figure 1c and 1e show non-redundant sensors failure. It can be seen that the redundant sensors failure does not change the difference coarray. While the non-redundant sensors failure, the virtual sensors in the difference coarray will have holes.

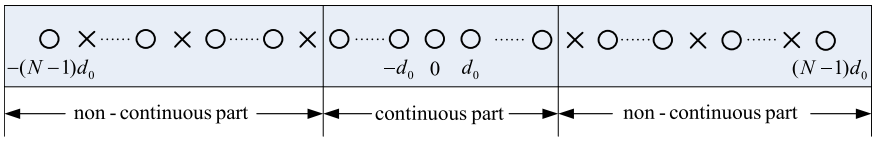


**FIGURE 2.** The difference coarray structure in non-redundant sensors failure scenarios for the ULA with N sensors. Virtual sensors are marked by hollow circles while the holes are depicted by crosses.

## III. DOA ESTIMATION METHOD IN SENSOR FAILURE SCENARIO

Based on the previous analysis, the different numbers and positions of failure sensors have crucial effects on DOA estimation performance, and also determine the choice of methods. In the case of redundant sensors failure, the missing elements in the covariance matrix can be recovered by using the difference coarray. We can use the continuous virtual sensors for DOA estimation by the MUSIC algorithm (CO-MUSIC).

In the case of non-redundant sensors failure, the difference coarray will have holes, and the numbers of available continuous virtual sensors will decrease, resulting in loss of DOFs, which may affects the applicability of CO-MUSIC. Even if the holes exist, there are other estimation methods, such as sparsity-based methods [34], [35] and coarry interpolation [36], that can be applied to the new difference coarray. However, these methods are usually computationally intensive, and the exact conditions and performance of the methods under different failure scenarios remain to be explored. Moreover, the sparsity-based method needs to discretize the angle domain, and there is a basis mismatch problem. We propose a covariance matrix reconstruction algorithm for DOA estimation in non-redundant sensors failure scenarios. The algorithm can increase the DOFs and maximum resolvable signal number by filling the virtual sensor holes in the discontinuous part of the difference coarray. Compared with the sparsity-based algorithms, this algorithm can eliminate the effect of the off-grid without discretization of the angle domain, and avoid regularization parameter selection. In addition, the proposed algorithm is also applicable to redundant sensors failure. The virtual sensors of remaining intact sensors can fill the positions of the failure sensors. Although the proposed algorithm does not increase the number of virtual sensors and DOFs, but by using Toeplitz covariance matrix reconstruction, the noise is effectively suppressed, and the accuracy is improved. Therefore, the proposed algorithm outperforms CO-MUSIC algorithm.

The covariance matrix of difference coarray shown in Figure 2 can be expressed as:

$$\boldsymbol{R} = \begin{bmatrix} \sum_{k=1}^{K}\sigma_k^2 & \sum_{k=1}^{K}\sigma_k^2 e^{-jO} & \cdots & \sum_{k=1}^{K}\sigma_k^2 e^{-jP} \\ \sum_{k=1}^{K}\sigma_k^2 e^{jO} & \sum_{k=1}^{K}\sigma_k^2 & \cdots & \sum_{k=1}^{K}\sigma_k^2 e^{-jQ} \\ \vdots & \vdots & \ddots & \vdots \\ \sum_{k=1}^{K}\sigma_k^2 e^{jP} & \sum_{k=1}^{K}\sigma_k^2 e^{jQ} & \cdots & \sum_{k=1}^{K}\sigma_k^2 \end{bmatrix} + \sigma_n^2 \boldsymbol{I}$$

$$= \begin{bmatrix} R(0) & R(-1) & \cdots & R(-(N-1)) \\ R(1) & R(0) & \cdots & R(-(N-2)) \\ \vdots & \vdots & \ddots & \vdots \\ R(N-1) & R(N-2) & \cdots & R(0) \end{bmatrix} + \sigma_n^2 \boldsymbol{I} \tag{10}$$

where $O = \pi \sin\theta_k, P = \pi(N-1)\sin\theta_k, Q = \pi(N-2)\sin\theta_k, \{R(d_u)\,|d_u = -(N-1), \cdots, (N-1)\}$ denotes the $2N-1$ different wave path differences. Note that $d_u$ is not continuous in the case of non-redundant sensors failure.

The difference coarray set according to the definition becomes:

$$D_u = \{-(N-1)d_0, \cdots, (N-1)d_0\} \tag{11}$$

According to (11) and (10), the elements in difference coarray denote the positions difference of each array sensor, corresponding to the wave path difference obtained by the covariance matrix. Note that, the elements in $D_u$ are not contiguous, which is caused by the holes in the difference coarray under non-redundant sensors failure scenarios.

Considering the influence of the signal-to-noise ratio (SNR) and the number of snapshots on the covariance matrix of the output data, the elements in the covariance matrix corresponding to the wave path difference in (10) are not completely equal, so the averaging operation is performed as:

$$\hat{R}(d_u) = \frac{1}{\omega_d(d_u)} \sum_{i=1}^{\omega_d(d_u)} R_i(d_u) \tag{12}$$

where $R_i(d_u)$ is the matrix element corresponding to the same wave path difference.

Based on the correspondence between the difference coarray and the wave path difference, the covariance matrix $\boldsymbol{R}$ is extended to a $N \times N$ Toeplitz covariance matrix with missing data, where some elements are zero,

$$R_{\mathrm{T}} = \begin{cases} \hat{R}(d_u), \text{ if } i-j = d_u, \\ 0, \text{ otherwise}, \end{cases} \tag{13}$$

$\boldsymbol{R}_{\mathrm{T}}$ can be equivalent to an output covariance matrix of an intact ULA, in which some elements are zero. We can fill the zero elements to get a virtual extended ULA covariance matrix.

Taking the 2nd, 4th, 5th, 7th, and 8th sensors failure of Fig. 1(e) as an example:

$$\boldsymbol{R} = \begin{bmatrix} R(0) & R(-1) & R(-5) & R(-6) & R(-9) \\ R(1) & R(0) & R(-4) & R(-5) & R(-8) \\ R(5) & R(4) & R(0) & R(-1) & R(-4) \\ R(6) & R(5) & R(1) & R(0) & R(-3) \\ R(9) & R(8) & R(4) & R(3) & R(0) \end{bmatrix} + \sigma_n^2 \boldsymbol{I} \tag{14}$$

We extend the covariance matrix $\boldsymbol{R}$ to a $10\times10$ Toeplitz covariance matrix $\boldsymbol{R}_{\mathrm{T}}$, as shown in (15), as shown at the bottom of this page.

In practical applications, the covariance matrix $\boldsymbol{R}$ is estimated with $L$ snapshots:

$$\hat{\boldsymbol{R}} = \frac{1}{L}\sum_{l=1}^{L}\boldsymbol{X}(t_l)\boldsymbol{X}^{\mathrm{H}}(t_l) \tag{16}$$

From (13), the estimate of $\hat{\boldsymbol{R}}_{\mathrm{T}}$ can be derived from the $\hat{\boldsymbol{R}}$ extension. Since the signal is sparse, $\boldsymbol{R}_{\mathrm{T}}$ is low rank. Using the matrix completion theory, the real $\boldsymbol{R}_{\mathrm{T}}$ can be obtained by solving the optimization problem. Under the limited snapshot condition, we achieve the fit between $\boldsymbol{R}_c$ and $\hat{\boldsymbol{R}}_{\mathrm{T}}$ through the second-order statistical properties. The covariance matrix can be recovered by the following formulation as:

$$\min \operatorname{rank}(\boldsymbol{R}_c),\ s.t.\ \left\|\hat{\boldsymbol{R}}_{\mathrm{T}}^{-\frac{1}{2}}\left(\hat{\boldsymbol{R}}_{\mathrm{T}}-\boldsymbol{R}_c\right)\hat{\boldsymbol{R}}_{\mathrm{T}}^{-\frac{1}{2}}\right\|_F^2 \le \eta, \boldsymbol{R}_c \ge 0 \tag{17}$$

where $\boldsymbol{R}_c$ represents the target matrix that needs to be reconstructed. $\eta$ is the predefined threshold.

It can be deduced that:

$$\begin{aligned}&\left\|\hat{\boldsymbol{R}}_{\mathrm{T}}^{-\frac{1}{2}}\left(\hat{\boldsymbol{R}}_{\mathrm{T}}-\boldsymbol{R}_c\right)\hat{\boldsymbol{R}}_{\mathrm{T}}^{-\frac{1}{2}}\right\|_F^2\\ &\quad=\operatorname{vec}^{\mathrm{H}}\left(\hat{\boldsymbol{R}}_{\mathrm{T}}-\boldsymbol{R}_c\right)\left(\hat{\boldsymbol{R}}_{\mathrm{T}}^{-\mathrm{T}}\otimes\hat{\boldsymbol{R}}_{\mathrm{T}}^{-1}\right)\operatorname{vec}\left(\hat{\boldsymbol{R}}_{\mathrm{T}}-\boldsymbol{R}_c\right)\\ &\quad=\left\|\hat{\boldsymbol{W}}^{-\frac{1}{2}}\operatorname{vec}\left(\hat{\boldsymbol{R}}_{\mathrm{T}}-\boldsymbol{R}_c\right)\right\|_2^2\end{aligned} \tag{18}$$

where $\hat{\boldsymbol{W}} = \frac{1}{L}\hat{\boldsymbol{R}}_{\mathrm{T}}^{\mathrm{T}}\otimes\hat{\boldsymbol{R}}_{\mathrm{T}}$.

Replacing the first constraint of (17) by (18), we can get:

$$\min \operatorname{rank}(\boldsymbol{R}_c),\ s.t.\ \left\|\hat{\boldsymbol{W}}^{-\frac{1}{2}}\operatorname{vec}\left(\hat{\boldsymbol{R}}_{\mathrm{T}}-\boldsymbol{R}_c\right)\right\|_2^2 \le \eta, \boldsymbol{R}_c \ge 0 \tag{19}$$

$\hat{\boldsymbol{R}}_{\mathrm{T}}$ is derived from the $\hat{\boldsymbol{R}}$ extension, and sensor failures cause multiple zero values in $\hat{\boldsymbol{R}}_{\mathrm{T}}$. The positions of the zero value provide none useful information. So we introduce the mapping matrix $\boldsymbol{P}$:

$$\min \operatorname{rank}(\boldsymbol{R}_c),\ s.t.\ \left\|\hat{\boldsymbol{W}}^{-\frac{1}{2}}\operatorname{vec}(\boldsymbol{P}\cdot(\hat{\boldsymbol{R}}_{\mathrm{T}}-\boldsymbol{R}_c))\right\|_2^2 \le \eta, \boldsymbol{R}_c \ge 0 \tag{20}$$

where $\boldsymbol{P}$ is the mapping matrix, and once the difference coarray is determined, the mapping matrix is constructed accordingly, which can be expressed as:

$$P(i,j) = \begin{cases}1, \text{ if } i-j=d_u,\\ 0, \text{ otherwise,}\end{cases} \tag{21}$$

According to the definition of the projection matrix $\boldsymbol{P}$, the position of the zero element in $\boldsymbol{P}$ is the same as that in $\hat{\boldsymbol{R}}_{\mathrm{T}}$. By introducing the matrix $\boldsymbol{P}$, the influence of the original zero element positions in $(\hat{\boldsymbol{R}}_{\mathrm{T}}-\boldsymbol{R}_c)$ is avoided.

In the model of (20), due to the non-convexity of the rank function, this problem is non-deterministic polynomial (NP-hard) problem and therefore difficult to solve. To avoid the non-convexity, we utilize convex relaxation to replace the rank norm with the nuclear norm. Since $\boldsymbol{R}_c$ is a positive semidefinite Hermitian matrix, the nuclear norm of $\boldsymbol{R}_c$ is equivalent to the trace norm of $\boldsymbol{R}_c$, that is, $\operatorname{tr}(\boldsymbol{R}_c)$ is used instead of $\operatorname{rank}(\boldsymbol{R}_c)$. Then the convex relaxation form of (20) is expressed as:

$$\min \operatorname{tr}(\boldsymbol{R}_c),\ s.t.\ \left\|\hat{\boldsymbol{W}}^{-\frac{1}{2}}\operatorname{vec}(\boldsymbol{P}\cdot(\hat{\boldsymbol{R}}_{\mathrm{T}}-\boldsymbol{R}_c))\right\|_2^2 \le \eta, \boldsymbol{R}_c \ge 0 \tag{22}$$

The $\boldsymbol{E} = \hat{R}_{\mathrm{T}}-\boldsymbol{R}_c$ satisfies the following asymptotic normal distribution.

*Proof:* Please see Appendix A.

$$\operatorname{vec}(\boldsymbol{E}) \sim \mathrm{AsN}(0, \boldsymbol{W}) \tag{23}$$

where $\boldsymbol{W} = \frac{1}{L}\boldsymbol{R}_c^{\mathrm{T}}\otimes\boldsymbol{R}_c$, $\boldsymbol{W}$ can be approximated by $\hat{\boldsymbol{W}} = \frac{1}{L}\hat{\boldsymbol{R}}_{\mathrm{T}}^{\mathrm{T}}\otimes\hat{\boldsymbol{R}}_{\mathrm{T}}$.

From (23) we can deduce the following formula:

$$\boldsymbol{W}^{-\frac{1}{2}}\operatorname{vec}(\boldsymbol{E}) \sim \mathrm{AsN}(0, \boldsymbol{I}_{N^2}) \tag{24}$$

then

$$\left\|\boldsymbol{W}^{-\frac{1}{2}}\operatorname{vec}(\boldsymbol{E})\right\|_2^2 \sim \mathrm{As}\chi^2(N^2) \tag{25}$$

where $\mathrm{As}\chi^2(N^2)$ is the chi-square distribution and the DOFs is $N^2$. Here, the parameter $\mu$ is introduced as follows:

$$\left\|\boldsymbol{W}^{-\frac{1}{2}}\operatorname{vec}(\boldsymbol{E})\right\|_2^2 \le \mu^2 \tag{26}$$

The probability that the true solution falls into the confidence interval $[0,\mu]$ is $\rho$, where $\rho$ is usually set to a very

$$\boldsymbol{R}_{\mathrm{T}} = \begin{bmatrix} R(0) & R(-1) & 0 & R(-3) & R(-4) & R(-5) & R(-6) & 0 & R(-8) & R(-9)\\ R(1) & R(0) & R(-1) & 0 & R(-3) & R(-4) & R(-5) & R(-6) & 0 & R(-8)\\ 0 & R(1) & R(0) & R(-1) & 0 & R(-3) & R(-4) & R(-5) & R(-6) & 0\\ R(3) & 0 & R(1) & R(0) & R(-1) & 0 & R(-3) & R(-4) & R(-5) & R(-6)\\ R(4) & R(3) & 0 & R(1) & R(0) & R(-1) & 0 & R(-3) & R(-4) & R(-5)\\ R(5) & R(4) & R(3) & 0 & R(1) & R(0) & R(-1) & 0 & R(-3) & R(-4)\\ R(6) & R(5) & R(4) & R(3) & 0 & R(1) & R(0) & R(-1) & 0 & R(-3)\\ 0 & R(6) & R(5) & R(4) & R(3) & 0 & R(1) & R(0) & R(-1) & 0\\ R(8) & 0 & R(6) & R(5) & R(4) & R(3) & 0 & R(1) & R(0) & R(-1)\\ R(9) & R(8) & 0 & R(6) & R(5) & R(4) & R(3) & 0 & R(1) & R(0) \end{bmatrix} + \sigma_n^2\boldsymbol{I} \tag{15}$$

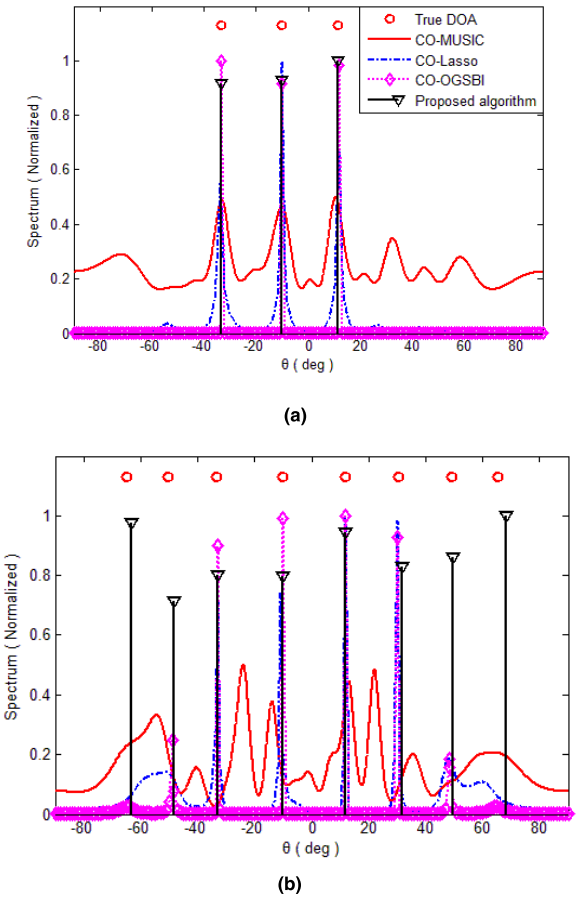


**FIGURE 3.** In the case of redundant sensors failure, the normalized spectrum of CO-MUSIC algorithm, CO-Lasso algorithm, CO-OGSBI algorithm and proposed algorithm for 3 sources and 8 sources respectively: (a) Normalized spectrum for 3 sources; (b) Normalized spectrum for 8 sources.

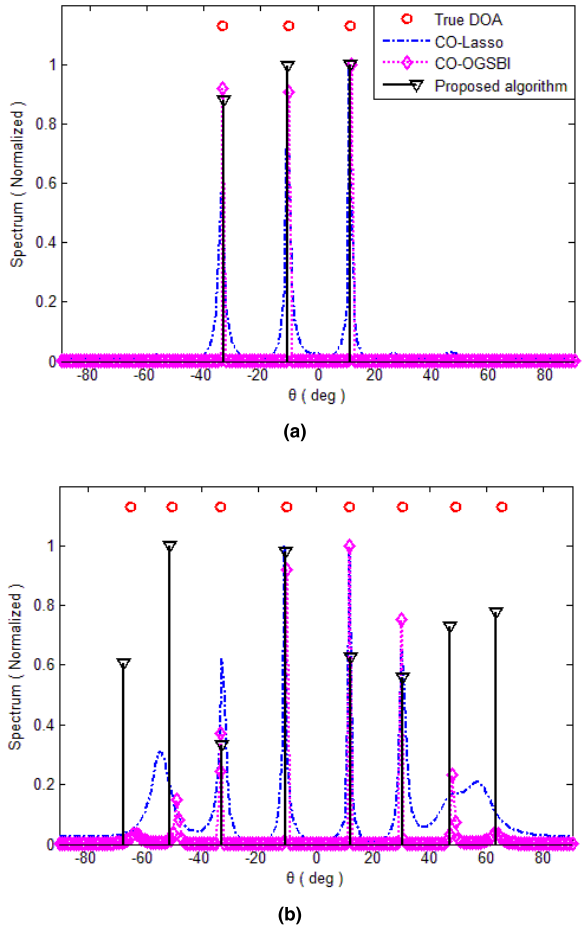


**FIGURE 4.** In the case of non-redundant sensors failure, the normalized spectrum of CO-Lasso algorithm, CO-OGSBI algorithm and proposed algorithm for 3 sources and 8 sources respectively: (a) Normalized spectrum for 3 sources; (b) Normalized spectrum for 8 sources.

large value such as 0.999. $\mu$ can be calculated by the function chi2inv$(\rho, N^2)$ which solves the chi-squared arrangement interval in Matlab.

We replace the constraint in (22) with (26), and then solve the following problem to recover the covariance matrix,

$$\min \mathrm{tr}(\boldsymbol{R}_c), s.t. \left\| \boldsymbol{W}^{-\frac{1}{2}} \mathrm{vec}(\boldsymbol{P} \cdot (\hat{\boldsymbol{R}}_{\mathrm{T}} - \boldsymbol{R}_c)) \right\|_2^2 \leq \mu^2, \boldsymbol{R}_c \geq 0 \tag{27}$$

The constraint minimization problem in (27) can be solved by optimization toolbox. The DOAs can be estimated from the optimal solution $\boldsymbol{R}_c$ by using the root-MUSIC algorithm.

In terms of computational complexity, the computational complexity of the proposed algorithm is approximately $\mathrm{O}\left(N^3 + LN_1^2 + N^2\right)$. The computational complexity of the CO-MUSIC is approximately $\mathrm{O}\left(LN_1^2 + N_2^3\right)$. For the CO-Lasso algorithm [34], the computational complexity is approximately $O\left(J^3 + \max\left(LN_1^2K, LN_1K^2\right)\right)$. For the OGSBI algorithm [37] combined with the difference coarray (CO-OGSBI), the computational complexity is approximately $O\left(\max\left(N_1J^2, LN_1J\right)\right)$. $J$ is the number of grids. $N$ is the number of sensors in intact ULA. $N_1$ is the number of sensors that have not failed. $N_2$ denotes the number of consecutive virtual sensors. In general, $J \gg N > K$. It can be seen that CO-MUSIC has the lowest computations, and the computational complexity of the proposed algorithm is lower than that of CO-Lasso and CO-OGSBI.

## IV. SIMULATION RESULTS

In this section, we use numerical simulations to verify the effectiveness of the proposed algorithm in scenarios where the numbers and positions of failure sensors are different. The performance of the proposed algorithm is compared with several DOA estimation algorithms in both overdetermined and underdetermined cases, including CO-MUSIC algorithm, CO-Lasso algorithm and CO-OGSBI algorithm. The intact ULA consists of 10 physical sensors. The angle search interval for setting the CO-MUSIC is 0.1°, and the sampling interval for the predefined spatial grid of the CO-Lasso and CO-OGSBI is set as 1°.

### A. SPATIAL SPECTRUM

We take 3 sources and 8 sources as examples, and assume that sources are far-field narrowband signals with equal power impinging on the array. In the case of 3 sources, the incident

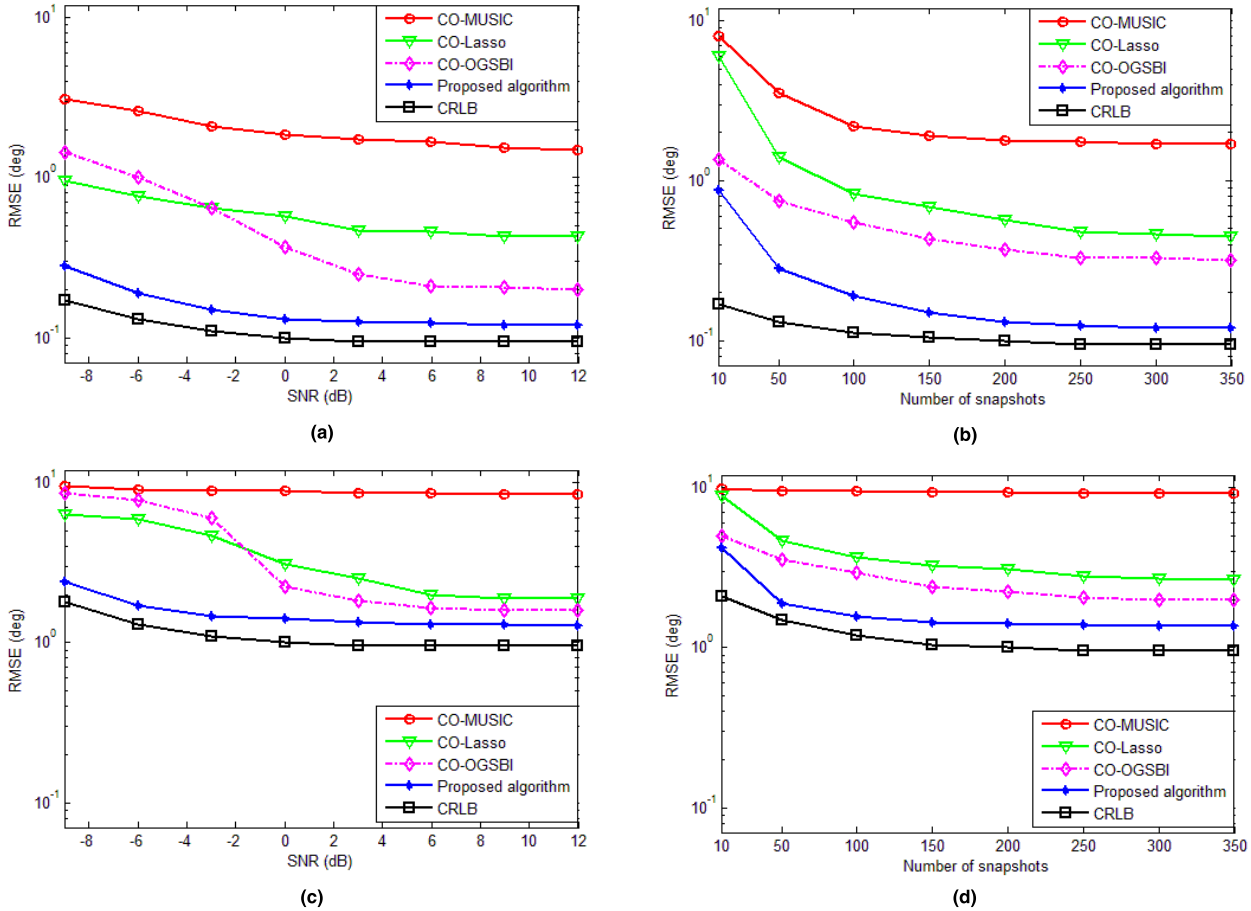


**FIGURE 5.** In the case of redundant sensors failure, the root mean square error (RMSE) of CO-MUSIC algorithm, CO-Lasso algorithm, CO-OGSBI algorithm and proposed algorithm for 3 sources and 8 sources respectively: (a) RMSE versus SNR for 3 sources, $L = 200$; (b) RMSE versus snapshots for 3 sources, SNR = 0dB; (c) RMSE versus SNR for 8 sources, $L = 200$; (d) RMSE versus snapshots for 8 sources, SNR = 0dB.

angle is $-33.43°$, $-10.19°$, 11.57 °, and in the case of 8 sources, the incident angle is -65.12°, $-50.34°$, $-33.43°$, $-10.25°$, 11.65°, 30.46°, 49.07°, 65.24°. The redundant sensors fail, taking the 2nd, 4th, 5th, 7th, and 8th sensors failure as an example. The remaining intact sensors are at $\{0d_0, 2d_0, 5d_0, 8d_0, 9d_0\}$. The CO-MUSIC, CO-Lasso, CO-OGSBI and the proposed algorithm are used to estimate DOA of 3 sources and 8 sources. The SNR is set to be 0 dB, and the number of snapshots is 300. The experimental results are shown in Figure 3. It can be seen that in the case of redundant sensors failure, all these algorithms can provide satisfactory DOA performance for 3 sources. When we perform DOA estimation on 8 sources, CO-MUSIC has poor performance and almost fails. CO-Lasso and CO-OGSBI are able to estimate the DOAs of a part of the sources, while the other part cannot be estimated. The proposed algorithm can still perform DOA estimation for each source.

The non-redundant sensors fail, taking the 3rd, 4th, 5th, 8th, and 9th sensors failure as an example. The remaining intact sensors are at $\{0d_0, 1d_0, 5d_0, 6d_0, 9d_0\}$. The SNR is set to be 0 dB, and the number of snapshots is 300. In this case, CO-MUSIC is completely invalid. The experimental results of CO-Lasso, CO-OGSBI and the proposed algorithm are shown in Figure 4. It indicates that CO-Lasso, CO-OGSBI and the proposed algorithm can give good estimation results of 3 sources. When we perform DOA estimation on 8 sources, CO-Lasso and CO-OGSBI can perform DOA estimation on a part of the sources, and another part of the sources cannot be estimated, while the proposed algorithm can still detect all the sources.

### B. RMSE VERSUS SNR AND SNAPSHOTS

We simulate the 3 sources and 8 sources in the case of redundant sensors failure and non-redundant sensors failure, and compare the RMSE performance of the four algorithms versus SNR and snapshots, performing 300 Monte Carlo experiments. In the case of 3 sources, the incident angle is -33.43° + $\Delta\theta$, -10.19° + $\Delta\theta$, 11.57 ° + $\Delta\theta$, and in the case of 8 sources, the incident angle is -65.12° + $\Delta\theta$, $-50.34°$ + $\Delta\theta$, $-33.43°$ + $\Delta\theta$, $-10.25°$ + $\Delta\theta$, 11.65° + $\Delta\theta$, 30.46° + $\Delta\theta$, 49.21° + $\Delta\theta$, 65.24° + $\Delta\theta$, where $\Delta\theta$ is chosen randomly from the interval $[-3°, 3°]$ in each trial to remove the possible prior information contained in the predefined direction set. The Cramér-Rao Lower Bound (CRLB) for the array geometry is also given as a benchmark. Figure 5 shows the

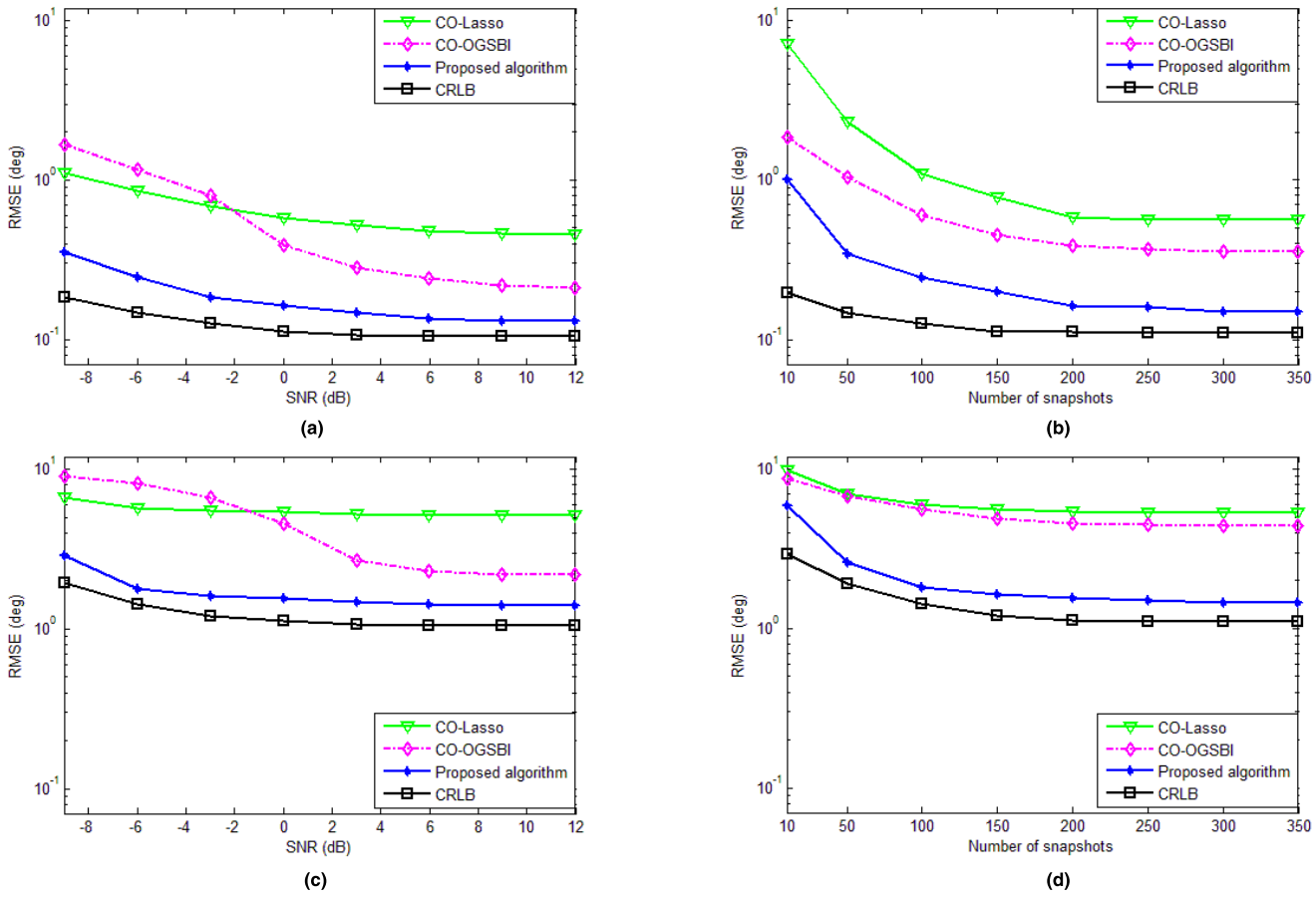


**FIGURE 6.** In the case of non-redundant sensors failure, the root mean square error (RMSE) of CO-Lasso algorithm, CO-OGSBI algorithm and proposed algorithm for 3 sources and 8 sources respectively: (a) RMSE versus SNR for 3 sources, $L = 200$; (b) RMSE versus snapshots for 3 sources, SNR = 0dB; (c) RMSE versus SNR for 8 sources, $L = 200$; (d) RMSE versus snapshots for 8 sources, SNR = 0dB.

RMSE performance of the four algorithms versus SNR and snapshots in the case of redundant sensors failure scenarios. As shown in Figure 5, when we perform DOA estimation in case of overdetermined, estimation errors of the four algorithms are small, and the proposed algorithm is much better. In the underdetermined condition, CO-MUSIC has poor performance and almost fails. CO-Lasso and CO-OGSBI have low RMSE when the SNR is high, and almost fails when the SNR is low, while the proposed algorithm can still obtain higher accuracy. The reason is that in the case of redundant sensors failure, the virtual sensors of remaining intact sensors can fill the positions of the failure sensors. Although the proposed algorithm does not increase the number of virtual sensors and DOFs, but by using covariance matrix reconstruction, the noise is effectively suppressed, and the estimation accuracy is improved. Therefore, the proposed algorithm outperforms CO-MUSIC, CO-Lasso and CO-OGSBI.

In the case of non-redundant sensors failure, CO-MUSIC is completely invalid. From Figure 6, in case of overdetermined, CO-Lasso, CO-OGSBI and the proposed algorithm can give good estimation accuracy, and the proposed algorithm performs better. The proposed algorithm has a significant advantage over CO-Lasso and CO-OGSBI in estimating accuracy in the underdetermined scenario. The reason is that the proposed algorithm can fill and utilize the virtual sensor holes, thus obtain more sensors and higher DOFs. Besides, the performance of CO-Lasso is degenerated as there is a basis mismatch caused by discretization of the angle domain. As a result, the proposed algorithm achieves the best performance.

### C. CPU TIME

The CPU time is defined as the runtime of each algorithm. We compare the CPU time of the four algorithms for 3 sources with the SNR varying from −15dB to 30dB. The simulation environment is Matlab 2014a, Intel Xeon E3 processor, 16 GB memory. The other parameter settings are the same as the redundant sensors failure in Simulation 1. Figure 7 shows the simulation results.

It can be concluded from Figure 7 that under the same simulation conditions, the CPU time required by the proposed algorithm is obviously less than CO-Lasso and CO-OGSBI, but more than CO-MUSIC. Nevertheless, it should be noted that, the increased computational cost of the proposed algorithm can be regard as a sacrifice for accuracy improvement.

Considering the analysis of the estimation accuracy, we can get a general conclusion: In the case of redundant sensors failure, the DOA estimation errors of the three algorithms are

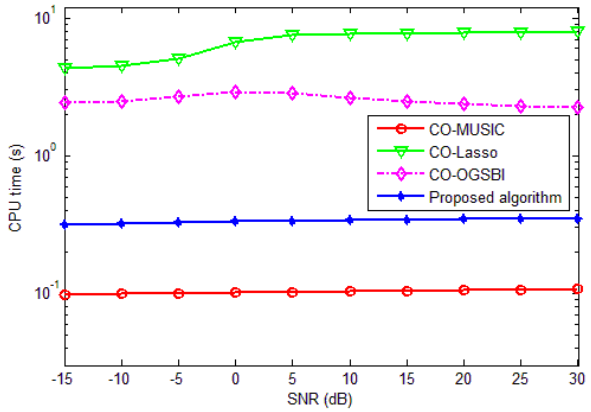


**FIGURE 7.** CPU time comparison of CO-MUSIC algorithm, CO-Lasso algorithm, CO-OGSBI algorithm and proposed algorithm.

small in the overdetermined condition, and CO-MUSIC with the fastest operation speed can be used when the accuracy is not strictly required. However, under the condition of underdetermined, CO-MUSIC has poor performance and basically invalid. The proposed algorithm is superior to CO-Lasso and CO-OGSBI in estimation accuracy and operation speed. Therefore, the proposed algorithm can be chosen. In the case of non-redundant sensors failure, CO-MUSIC is invalid, and the estimated performance of CO-Lasso and CO-OGSBI is significantly degraded. The proposed algorithm outperforms CO-Lasso and CO-OGSBI in estimation accuracy and operation speed. Therefore, the proposed algorithm is the optimal choice for non-redundant sensors failure.

## V. CONCLUSION

Array sensors failure can significantly deteriorate the performance of DOA estimation. To address this problem, we propose a covariance matrix reconstruction algorithm for DOA estimation. In the first stage, we devise a diagnosis method to detect the failure sensors. Then we classify the failure sensors into redundant sensors and non-redundant sensors. In the second stage, the former can be solved by using the virtual sensors to occupy the positions of failure sensors. As for the latter, the covariance matrix is extended to a high-dimensional Toeplitz matrix with missing data. We employ the mapping matrix, further use trace norm instead of the rank norm for convex relaxation to reconstruct the covariance matrix, thereby realizing the filling of the virtual sensor holes in the difference coarray and restoring the DOFs. Numerical experiments demonstrate the superiority of the proposed algorithm as compared to some of the existing algorithm, especially in the case of non-redundant sensors failure.

## APPENDIX A

*Proof:* $\boldsymbol{E} = \hat{R}_{\mathrm{T}} - \boldsymbol{R}_c$, Let $\Phi = vec(\boldsymbol{E})$. Prove that $\Phi$ satisfies the following asymptotic normal distribution.

$$\Phi \sim \mathrm{AsN}(0, \frac{1}{L}\boldsymbol{R}_c^{\mathrm{T}} \otimes \boldsymbol{R}_c) \tag{28}$$

We assume that the $(m,p) - th$ element of the sample covariance matrix $\hat{\boldsymbol{R}}_{\mathrm{T}}$ is $\hat{r}_{m,p}$. The $(m,p) - th$ element of the target matrix $\boldsymbol{R}_c$ is $r_{m,p}$, we have:

$$\begin{aligned}\hat{r}_{m,p} &= \frac{1}{L}\sum_{t=1}^{L} x_m(t)x_p^*(t) \\ &= \frac{1}{L}\sum_{t=1}^{L} (\boldsymbol{A}[m,:]\boldsymbol{S}(t) + n_m(t))(\boldsymbol{A}[p,:]\boldsymbol{S}(t) + n_p(t))^*\end{aligned} \tag{29}$$

Also assuming that both the source signals and the noises are uncorrelated, we can get:

$$\boldsymbol{E}\left\{\hat{r}_{m,p}\right\} = \boldsymbol{A}[m,:]\boldsymbol{R}_{\boldsymbol{S}}\boldsymbol{A}[p,:] + \delta_{m,p}\sigma_n^2 = r_{m,p} \tag{30}$$

and

$$\begin{aligned}&\boldsymbol{E}\left\{(\hat{r}_{m,p} - r_{m,p})(\hat{r}_{k,l} - r_{k,l})^*\right\} \\ &= \frac{1}{L^2}\sum_{t_1=1}^{L}\sum_{t_2=1}^{L}\boldsymbol{E}\left\{(\boldsymbol{A}[m,:]\boldsymbol{S}(t_1) + n_m(t_1))\right. \\ &\quad \times \left(\boldsymbol{A}[p,:]\boldsymbol{S}(t_1) + n_p(t_1)\right)^* \\ &\quad \left.\cdot (\boldsymbol{A}[k,:]\boldsymbol{S}(t_2) + n_k(t_2))^*\,(\boldsymbol{A}[l,:]\boldsymbol{S}(t_2) + n_l(t_2))\right\} - r_{m,p}r_{k,l}^* \\ &= \frac{1}{L^2}\sum_{\substack{t_1=1\\ t_1\neq t_2}}^{L}\sum_{t_2=1}^{L}\boldsymbol{E}\left\{\cdots\right\} + \frac{1}{L^2}\sum_{t_1=t_2=1}^{L}\boldsymbol{E}\left\{\cdots\right\} - r_{m,p}r_{k,l}^*\end{aligned} \tag{31}$$

The ellipsis of $\boldsymbol{E}\{\cdots\}$ represents the expected part after the first equal sign in (31).
where

$$\frac{1}{L^2}\sum_{\substack{t_1=1\\ t_1\neq t_2}}^{L}\sum_{t_2=1}^{L}\boldsymbol{E}\left\{\cdots\right\} = \frac{L^2 - L}{L^2}r_{m,p}r_{k,l}^* \tag{32}$$

and

$$\frac{1}{L^2}\sum_{t_1=t_2=1}^{L}\boldsymbol{E}\left\{\cdots\right\} = \frac{1}{L}(r_{m,p}r_{k,l}^* + r_{m,k}r_{l,p}) \tag{33}$$

We thus get:

$$\boldsymbol{E}\left\{(\hat{r}_{m,p} - r_{m,p})(\hat{r}_{k,l} - r_{k,l})^*\right\} = \frac{r_{m,k}r_{l,p}}{L} \tag{34}$$

then

$$\boldsymbol{E}\left\{\Phi\Phi^{\mathrm{H}}\right\} = \frac{1}{L}\boldsymbol{R}_c^{\mathrm{T}} \otimes \boldsymbol{R}_c \tag{35}$$

This completes the proof.

## REFERENCES

[1] A. B. Gershman, M. Rübsamen, and M. Pesavento, "One- and two-dimensional direction-of-arrival estimation: An overview of search-free techniques," *Signal Process.*, vol. 90, no. 5, pp. 1338–1349, 2010.
[2] X. Wang, W. Wei, X. Li, and J. Liu, "Real-valued covariance vector sparsity-inducing DOA estimation for monostatic MIMO radar," *Sensors*, vol. 15, no. 11, pp. 28271–28286, Nov. 2015.

[3] J. Shi, G. Hu, X. Zhang, and F. Sun, "Sparsity-based DOA estimation of coherent and uncorrelated targets with flexible MIMO radar," *IEEE Trans. Veh. Technol.*, vol. 68, no. 6, pp. 5835–5848, Jun. 2019.

[4] L. C. Godara, "Application of antenna arrays to mobile communications. II. Beam-forming and direction-of-arrival considerations," *Proc. IEEE*, vol. 85, no. 8, pp. 1195–1245, Aug. 1997.

[5] A. Moffet, "Minimum-redundancy linear arrays," *IEEE Trans. Antennas Propag.*, vol. AP-16, no. 2, pp. 172–175, Mar. 1968.

[6] P. Pal and P. P. Vaidyanathan, "Nested arrays: A novel approach to array processing with enhanced degrees of freedom," *IEEE Trans. Signal Process.*, vol. 58, no. 8, pp. 4167–4181, Aug. 2010.

[7] J. Shi, G. Hu, X. Zhang, F. Sun, and H. Zhou, "Sparsity-based two- dimensional DOA estimation for coprime array: From sum-difference coarray viewpoint," *IEEE Trans. Signal Process.*, vol. 65, no. 21, pp. 5591–5604, Nov. 2017.

[8] M. Wang and A. Nehorai, "Coarrays, music, and the cramér–rao bound," *IEEE Trans. Signal Process.*, vol. 65, no. 4, pp. 933–946, Feb. 2017.

[9] P. Gupta and M. Agrawal, "Design and analysis of the sparse array for DOA estimation of noncircular signals," *IEEE Trans. Signal Process.*, vol. 67, no. 2, pp. 460–473, Jan. 2019.

[10] C.-L. Liu and P. P. Vaidyanathan, "Robustness of difference coarrays of sparse arrays to sensor failures—Part I: A theory motivated by coarray MUSIC," *IEEE Trans. Signal Process.*, vol. 67, no. 12, pp. 3213–3226, Jun. 2019.

[11] C.-L. Liu and P. P. Vaidyanathan, "Robustness of difference coarrays of sparse arrays to sensor failures—Part II: Array geometries," *IEEE Trans. Signal Process.*, vol. 67, no. 12, pp. 3227–3242, Jun. 2019.

[12] W. Zheng, X. Zhang, P. Gong, and H. Zhai, "DOA estimation for coprime linear arrays: An ambiguity-free method involving full DOFs," *IEEE Commun. Lett.*, vol. 22, no. 3, pp. 562–565, Mar. 2018.

[13] Q. Xie, X. Pan, and S. Xiao, "Enhance degrees of freedom for coprime array using optspace algorithm," *IEEE Access*, vol. 7, pp. 32672–32680, 2019.

[14] J. Shi, G. Hu, X. Zhang, F. Sun, W. Zheng, and Y. Xiao, "Generalized co-prime MIMO radar for DOA estimation with enhanced degrees of freedom," *IEEE Sensors J.*, vol. 18, no. 3, pp. 1203–1212, Feb. 2018.

[15] B. Yao, Z. Dong, W. Zhang, W. Wang, and Q. Wu, "Degree-of-freedom strengthened cascade array for DOD-DOA estimation in MIMO array systems," *Sensors*, vol. 18, no. 5, p. 1557, May 2018.

[16] B. K. Yeo and Y. Lu, "Expeditious diagnosis of linear array failure using support vector machine with low-degree polynomial kernel," *IET Microw., Antennas Propag.*, vol. 6, no. 13, pp. 1473–1480, Oct. 2012.

[17] B.-K. Yeo and Y. Lu, "Array failure correction with a genetic algorithm," *IEEE Trans. Antennas Propag.*, vol. 47, no. 5, pp. 823–828, May 1999.

[18] H. Zhao, Y. Zhang, E. P. Li, A. Buonanno, and M. D'Urso, "Diagnosis of array failure in impulsive noise environment using unsupervised support vector regression method," *IEEE Trans. Antennas Propag.*, vol. 61, no. 11, pp. 5508–5516, Nov. 2013.

[19] K. T. Wong, Y. I. Wu, Y.-S. Hsu, and Y. Song, "A lower bound of DOA-estimates by an array randomly subject to sensor-breakdown," *IEEE Sensors J.*, vol. 12, no. 5, pp. 911–913, May 2012.

[20] S. Vigneshwaran, N. Sundararajan, and P. Saratchandran, "Direction of arrival (DOA) estimation under array sensor failures using a minimal resource allocation neural network," *IEEE Trans. Antennas Propag.*, vol. 55, no. 2, pp. 334–343, Feb. 2007.

[21] O. M. Bucci, M. D. Migliore, G. Panariello, and P. Sgambato, "Accurate diagnosis of conformal arrays from near-field data using the matrix method," *IEEE Trans. Antennas Propag.*, vol. 53, no. 3, pp. 1114–1120, Mar. 2005.

[22] T. Ince and G.Ögücü, "Array failure diagnosis using nonconvex compressed sensing," *IEEE Antennas Wireless Propag. Lett.*, vol. 13, no. 9, pp. 992–995, Jan. 2015.

[23] N. Singh, M. Rattan, and M. S. Patterh, "A linear antenna array failure correction using improved bat algorithm," *Int. J. RF Microw. Comput. Aided Eng.*, vol. 27, no. 7, Apr. 2017, Art. no. e21119.

[24] N. S. Grewal, M. Rattan, and M. S. Patterh, "A non-uniform circular antenna array failure correction using firefly algorithm," *Wireless Pers. Commun.*, vol. 97, no. 10, pp. 845–858, May 2017.

[25] S. U. Khan, M. K. A. Rahim, and L. Ali, "Correction of array failure using grey wolf optimizer hybridized with an interior point algorithm," *Front. Inform. Technol. Electron. Eng.*, vol. 19, no. 9, pp. 1191–1202, Sep. 2018.

[26] W. Y. Zhang, S. A. Vorobyov, and L. H. Guo, "DOA estimation in MIMO radar with broken sensors by difference co-array processing," in *Proc. IEEE Int. Workshop Comput. Adv. Multi-Sensor Adapt. Process.*, Dec. 2015, pp. 321–324.

[27] C. L. Zhu, W. Q. Wang, H. Chen, and H. C. So, "Impaired sensor diagnosis, beamforming and DOA estimation with difference Co-Array processing," *IEEE Sensors J.*, vol. 15, no. 7, pp. 3773–3780, Jul. 2015.

[28] X. M. Wang and X. Wang, "Hole identification and filling in k-times extended co-prime arrays for highly efficient DOA estimation," *IEEE Trans. Signal Process.*, vol. 67, no. 10, pp. 2693–2706, May 2019.

[29] M. Yang, A. M. Haimovich, X. Yuan, L. Sun, and B. Chen, "A unified array geometry composed of multiple identical subarrays with hole-free difference coarrays for underdetermined DOA estimation," *IEEE Access*, vol. 6, pp. 14238–14254, 2018.

[30] S. M. Hosseini and M. A. Sebt, "Array interpolation using covariance matrix completion of minimum-size virtual array," *IEEE Signal Process. Lett.*, vol. 24, no. 7, pp. 1063–1067, Jul. 2017.

[31] Y. Hu, D. Zhang, J. Ye, X. Li, and X. He, "Fast and accurate matrix completion via truncated nuclear norm regularization," *IEEE Trans. Pattern Anal. Mach. Intell.*, vol. 35, no. 9, pp. 2117–2130, Sep. 2013.

[32] X.-H. Wu, W.-P. Zhu, and J. Yan, "A Toeplitz covariance matrix reconstruction approach for direction of arrival estimation," *IEEE Trans. Veh. Technol.*, vol. 66, no. 9, pp. 8223–8237, Sep. 2017.

[33] A. Alexiou and A. Manikas, "Investigation of array robustness to sensor failure," *J. Franklin I.*, vol. 342, no. 3, pp. 255–272, May 2005.

[34] Y. D. Zhang, S. Qin, and M. G. Amin, "DOA estimation exploiting coprime arrays with sparse sensor spacing," in *Proc. IEEE Int. Conf. Acoust., Speech Signal Process.*, May 2014, pp. 2267–2271.

[35] P. Pal and P. P. Vaidyanathan, "Pushing the limits of sparse support recovery using correlation information," *IEEE Trans. Signal Process.*, vol. 63, no. 3, pp. 711–726, Feb. 2015.

[36] Y. I. Abramovich, N. K. Spencer, and A. Y. Gorokhov, "Positive-definite Toeplitz completion in DOA estimation for nonuniform linear antenna arrays. II. Partially augmentable arrays," *IEEE Trans. Signal Process.*, vol. 47, no. 6, pp. 1502–1521, Jun. 1999.

[37] Z. Yang, L. Xie, and C. Zhang, "Off-grid direction of arrival estimation using sparse Bayesian inference," *IEEE Trans. Signal Process.*, vol. 61, no. 1, pp. 38–43, Jan. 2013.

**BING SUN** was born in Anhui, China, in 1991. He received the B.S. and M.S. degrees from the Electronic Engineering Institute, Hefei, China, in 2014 and 2016, respectively. He is currently pursuing the Ph.D. degree with the National University of Defense Technology, Hefei.

His fields of interests include spatial information processing, array signal processing, and radar countermeasure theory.

**CHENXI WU** was born in Anhui, China, in 1988. He received the M.S. and Ph.D. degrees from the Electronic Engineering Institute, Hefei, China, in 2014 and 2017, respectively. He is currently a Lecturer with the National University of Defense Technology.

His research interests include array signal processing, spatial information processing, and sparse reconstruction technology.

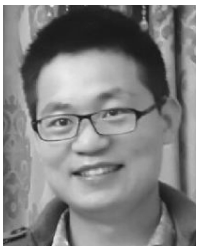

**JUNPENG SHI** received the M.Sc. and Ph.D. degrees from Air Force Engineering University, Xi'an, China, in 2014 and 2018, respectively. He is currently a Lecturer in information and communication engineering with the National University of Defense Technology (NUDT), Hefei, China.

His current research interest is mainly focused on tensor signal processing with sparse MIMO radar.

**HUAI-LIN RUAN** was born in Anhui, China, in 1964. He received the B.S. and M.S. degrees from the Electronic Engineering Institute, Hefei, China, in 1990 and 1993, respectively, and the Ph.D. degree from the Institute of Plasma Physics, Chinese Academy of Sciences, Hefei, in 2001. He is currently a Professor with the National University of Defense Technology.

He has been doing research in the fields of array signal processing, spatial information processing, radar countermeasure theory, and compressed sensing theory.

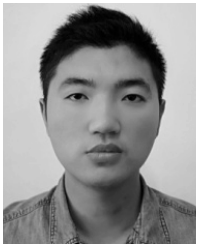

**WEN-QIANG YE** was born in Anhui, China, in 1994. He received the B.S. degree from the Xiamen University, in 2016, and the M.S. degree from the National University of Defense Technology, in 2018. His general research interests include deep learning and radar signal processing.